Universal Journal of Applied Science 6(1): 1-8, 2019
DOI: 10.13189/ujas.2019.060101 http://www.hrpub.org

A Method to Improve the Performance of Gold Nanoparticle Suspensions for Trace Detection of 16 EPA Priority PAHs

Anna Kolomijeca[1,2]

[1]Department of Ecology and Evolutionary biology, University of Toronto, Canada
[2]Department of Mechanical and Industrial Engineering, University of Toronto, Canada

Abstract The growing demand for fast, simple and inexpensive analytical techniques to investigate environmental pollution has resulted in a large number of studies where surface enhanced Raman spectroscopy is used to detect environmental contaminants. However, extraction of weak Raman spectra from complex background signals remains challenging. In this current work, the author has presented a method to improve the performance of gold nanoparticles suspensions for trace detection of the 16 EPA priority PAHs. The gold nanoparticles in suspension are first mixed with the analyte in the liquid phase and then transferred to a solid state by drying (as opposed to liquid sample + dry substrate or liquid sample + liquid substrate). This method allows for a complete background signal removal (including fluorescence and signal from the substrate), strong Raman signal enhancement from the analyte and a reduction in substrate preparation time. Performance of a developed substrate (CNP-Au) was compared with a commercially available 3D substrate (Ram-SERS-Au) by measuring of all 16 EPA priority PAHs. The developed CNP-Au substrate exhibited experimentally obtained LODs three orders of magnitude lower than Ram-SERS-Au, down to the range of 1 ppb. The standard deviation of signal reproducibility for CNP-Au is 14%. Ram-SERS-Au and CNP-Au were characterized using SEM imaging.

Keywords SERS Suspensions, Priority PAHs, Gold Nanoparticles, Raman

1. Introduction

Polycyclic aromatic hydrocarbons (PAHs) are common environmental pollutants with toxic, mutagenic and/or carcinogenic properties [1]. Identification of PAHs in environmental samples is essential for understanding their prevalence and impacts. Raman spectroscopy allows one to obtain a "fingerprint" of information of a chemical(s) within seconds. However, when measuring PAHs at environmentally-relevant concentrations, the signal is too weak to be detected [2] due to a low Raman scattering cross section. The application of Surface Enhanced Raman Spectroscopy (SERS) can increase measurement sensitivity up to a factor of 10^7 [3]. The electromagnetic enhancement mechanism is dominant in SERS [4] and occurs due to the concentration of electromagnetic field associated with light in nanostructured electronically-conducting materials (such as silver or gold), followed by excitation of surface plasmons (SP) that resonantly emit radiation from nearby molecules [5]. Nanoparticles morphology and degree of aggregation will dictate SERS efficiency, since junctions between the particles will serve as SERS hot spots, enabling single molecule detection [6]. Typically three types of nanoparticles are used for SERS: nanospheres, nanotriangles and nanostars [7], as well as three types of substrates: (1) metal nanoparticles in suspension [8]; (2) metal nanoparticles immobilized on solid-support substrate (prepared by bottom-up methods, such as wet chemistry [6], [9], [10]) and (3) nanostructures fabricated directly on solid-support substrates (generally prepared by a top-down methods, such as lithography-based fabrication [11], [12], [13] or templating [14]). Most of the studies that have been done on PAH detection with SERS apply solid-support substrates prepared by bottom-up approach [15], [16], [9], [17], [18], [19], [20], [21], [22], [23] due to the low production costs, good substrate performance and high reproducibility. However, this requires preparation of a new substrate before each measurement, which can be time-consuming. Shi et al [24] applies gold nanoparticles suspension to detect five different PAHs. However, presented measurements strongly suffer from background

noise. In fact, extracting weak Raman spectra from a complex background signal has been a significant challenge for all above studies. For example, in the studies of Bao et al [21] and Shi et al [24], [25], the signal from the analyte (in LOD concentrations) cannot be seen without the magnification of the specific spectral area due to strong background noise. This causes problems measuring untargeted samples, as it is important to observe more than one peak to determine chemicals present.

Several methods exist to extract the Raman spectra from the background noise: a) reducing fluorescence of the sample by photobleaching [26], fluorescence quenching[27], sample washing or filtration [28] (only possible for some samples), b) manipulating Raman scattering properties, such as using longer wavelengths, or anti-Stokes Raman spectroscopy (which produces a lower Raman signal response); c) application of computational methods, such as baseline correction, background extraction (which can be efficient for the initial substrate-spectra removal, but less efficient for autofluorescence correction); d) application of dual laser measurements in combination with computational technique, such as shifted excitation Raman difference spectroscopy (SERDS) [29] (which requires sophisticated equipment).

Because the current study deals with persistent organic pollutants that are relatively stable, the author applies a heat treatment technique (excess liquid evaporation) on a sample to completely eliminate fluorescence and background noise.

Typically, an analyte is added to a nanoparticle suspension or applied on the top of solid-support substrate and measured as liquid + liquid or solid + liquid (in case liquid sample is dried on the top of the solid substrate, the sample will cover only a top layer of the substrate). In this study, the analyte is first mixed with the nanoparticle suspension (liquid + liquid) then dried until solid (a glass slide can serve as a substrate base). This simple and new substrate/sample processing method allows encapsulating the sample inside the structure of the substrate, ensuring better interaction between the sample and gold nanoparticles and resulting in lower LODs. To the knowledge of the author, such an approach has not been used before. The advantages of this method are: a) concentration of the sample due to excess liquid extraction; b) background noise and fluorescence removal due to evaporation of the solvents from the substrate and the sample; c) low production costs; d) the ability to use the same nanoparticles suspension for numerous measurements without the need to prepare a "fresh" substrate every time (relevant to solid-support substrates).

In this study, the author presents experimentally obtained LODs for all 16 EPA priority PAHs, when at least half of the characteristic Raman peaks can be clearly observed without manipulating the spectrum. The SERS performance of a developed substrate (CNP-Au) is compared to a commercial 3D (Ram-SERS-Au) substrate. Both substrates are characterized by scanning electron microscopy imaging.

2. Materials and Methods

2.1. Preparation of SERS Substrates

A clustered gold nanoparticle suspension (CNP-Au) was prepared by Ocean Optics with the following procedure. Gold (III) chloride hydrate (HAuCl4) and sodium citrate tribasic dehydrate were purchased from Sigma-Aldrich. The colloidal gold nanoparticle suspension consists of 50 nm diameter gold nanospheres in water that exhibit a surface plasmon resonance (SPR) absorption band of ~ 785 nm. Spherical gold nanoparticles were synthesized according to the method of Lee and Meisel [30]. Briefly, 0.8 ml of 0.294 M HAuCl4 was added to 400 ml of purified water and heated to a vigorous boil in a beaker. At this point, 120 mg of sodium citrate in 1 ml of water was added to the gold solution, where the solution changes from colorless to reddish-purple within minutes, indicating the formation of gold nanoparticles. After stirring and boiling for 15 minutes, the solution is removed from heat and allowed to cool overnight before further processing. The CNP-Au solution can be stored in the fridge up to 1 year (longer term was not experimentally tested). Before each measurement 50 µl of CNP-Au solution is mixed with, 50 µl of the analyte on the top of a glass slide (or petri dish) and placed in the oven at 45^{o} C for 1h to allow for liquid evaporation and crystal formation.

Quartz fiber embedded gold nanoparticles (Ram-SERS-Au) were prepared by Ocean Optics according to a method developed by Hoppmann et al. Gold nanoparticles were concentrated 100 times, removing the supernatant and redispersing the pellet in a 5:4:1 nanoparticles:glycerol:ethanol mixture [31]. Next, a few microliters of the formulated ink was deposited on quartz paper substrates pre-cut into 8 mm diameter circles and allowed to dry. The substrates are made of 50 nm diameter gold nanospheres deposited on 8 mm diameter quartz paper circles.

2.2. Chemicals and Solutions

All PAHs were purchased from Sigma-Aldrich. Acenaphthene, acenaphthylene, anthracene, benzo[a]pyrene, dibenz[a,h]anthracene, fluoranthene, fluorene, Indeno[1,2,3-cd]pyrene, naphthalene, pyrene, phenanthrene and fluoranthene were in a powder state and dissolved in methanol (Fisher chemical, 99.9%) in concentrations of 1000 ppm (stock solution), 100 ppm (diluted), 10 ppm (diluted), 1 ppm (diluted) and 0.1 ppm (diluted). Stock solutions were made based on the following calculations:

$$C_{ppm}=10^6 \cdot C_{g/l}/\rho_{(kg/m^3)}$$

where C is concentration and ρ is solution density.

Bnzo[ghi]perylene (in methylene chloride), benzo[k]fluoranthene (powder) and crysene (powder) were dissolved in acetone (from Fisher Chemical) in the same concentrations as above. Benz[a]anthracene (1000µg/ml) and Benzo[b]fluoranthene (200µg/ml) came already in methanol solution. After this preparation, all the solutions were stored in a freezer at –20° C.

2.3. Instrumentation

Microbalance scales from Mettler Toledo XP6 model were used to weigh PAHs.

All SERS measurements were recorded at room temperature using a commercially available Raman microscope, Xplora Plus by HORIBA France SAS. The laser beam was focused through a standard x50 objective with 1.9 µm laser spot size. All Raman/SERS spectra were recorded with an excitation wavelength of 785 nm, beam filter of 10%, and 10mW laser power. The laser beam exposure time was 10 s, and accumulation of 10. The intensity of the Raman peak at 520 cm^{-1} from silicon was normalized before each data acquisition. Data was analyzed using LabSpec 6.

3. Results

3.1. Characterization of SERS Substrates

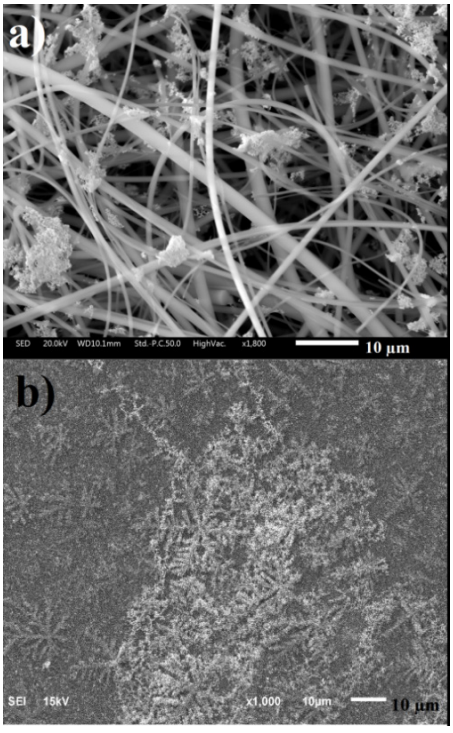

Figure 1. Scanning electron microscopy image of the surface enhanced Raman scattering substrate a) Quartz fiber embedded gold nanoparticles (Ram-SERS-Au); b) Clustered gold nanoparticles in the solid phase (CNP-Au), prepared before each measurement by evaporating the liquid from gold nanoparticles suspension.

Scanning Electron Microscopy (SEM) images were taken to characterize the SERS surfaces. Figure 1a displays the surface morphology of the conventional solid-support RAM-SERS-Au substrate. As can be seen, gold nanoparticles are self-assembled in clusters and dispersed around quartz fibers in 3D space. Such particle distribution provides high density hot spots, thus enhancing the SERS signal. In contrast, a more efficient way to create higher density hot spot areas is to allow gold particles to self-assemble into crystals (CNP-Au substrate), which is shown in Figure 1b. All the gold particles are grouped into 3D clustered crystals, providing an enormous number of hot spots. Since the CNP-Au substrate doesn't have a uniform homogeneity, in order to achieve optimal results, the SERS measurements were performed with the laser beam focused on the crystals.

3.2. Raman Signal Extraction

The evaporation of the excess liquid from the sample allows strong enhancement of the Raman signal. Figure 2a shows Raman measurements of 1 ppm pyrene in methanol, which is mixed with CNP-Au substrate (50:50) in a liquid form. The signal from pyrene is too weak to be detected. After the drying process, all major pyrene peaks can be clearly observed with practically no background noise (figure 2b). Four Raman peaks from pyrene at 406 cm^{-1} (C-C-C bending), 589 cm^{-1} (C-C-C bending), 1235 cm^{-1} (C-C stretching) and 1401 cm^{-1} (C-C stretching) closely correspond with that of solid pyrene (see table 1), while the 1609 cm^{-1} peak has been strongly shifted compared to the 1625cm^{-1} of a solid pyrene. Such shifts can occur during photochemical reactions upon irradiation by the laser, when the pyrene is absorbed onto gold colloidal nanoparticles [24].

3.3. Limits of Detection

Since the focus of this work is to demonstrate a suitability of the suspension method for potential non-targeted analysis, it is essential to observe at least half of the characteristic Raman peaks in the sample. An example of determining LOD for one PAH, fluoranthene, at six different concentrations in methanol using conventional Ram-SERS-Au substrates and CNP-Au substrate (prepared by suspension method) is shown in figure 3. As we can observe, LOD of fluoranthene for CNP-Au (figure 3a) is an order of magnitude lower (0.1 ppm) than for Ram-SERS-Au (1 ppm, figure 3b). Note, that "blank" spectra of the CNP-Au substrate (figure 3a, "0 ppm") does not produce any additional signals compared to the "blank" measurement of Ram-SERS-Au (figure 3b, "0 ppm"). This is due to the evaporation of the solvents and other chemicals during the substrate drying process.

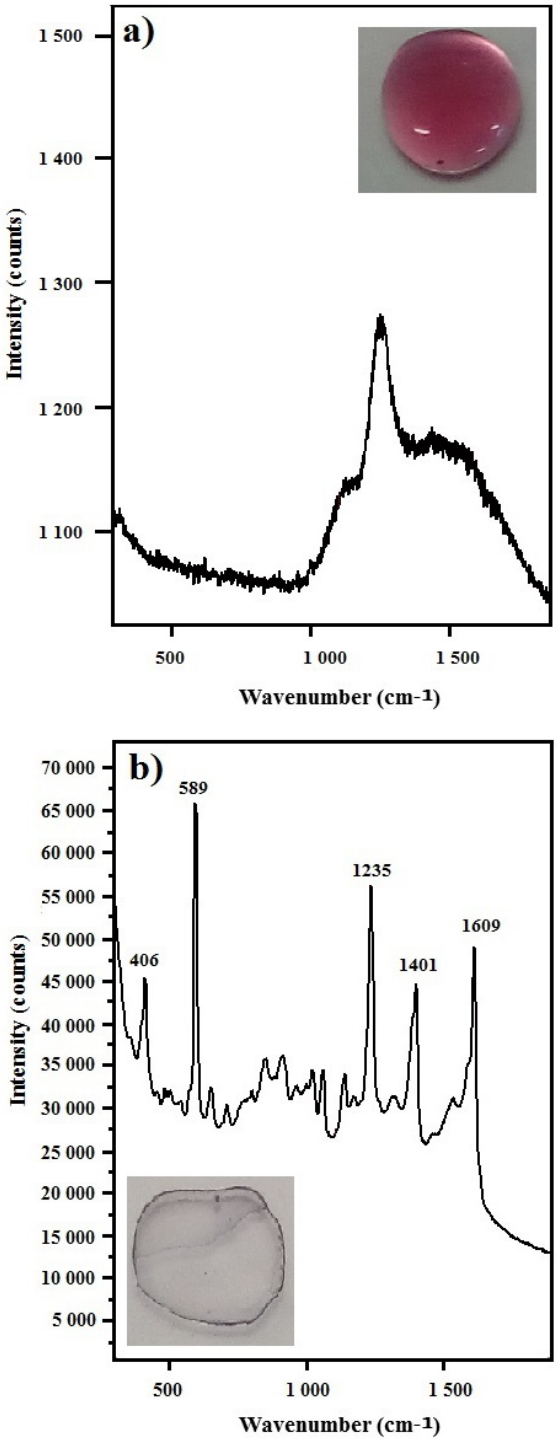

Figure 2. Spectrum of 1 ppm pyrene in MeOH on CNP-Au substrate in a) liquid state, b) dried form. Λ=785nm, laser power 10 mW, integration time 10s

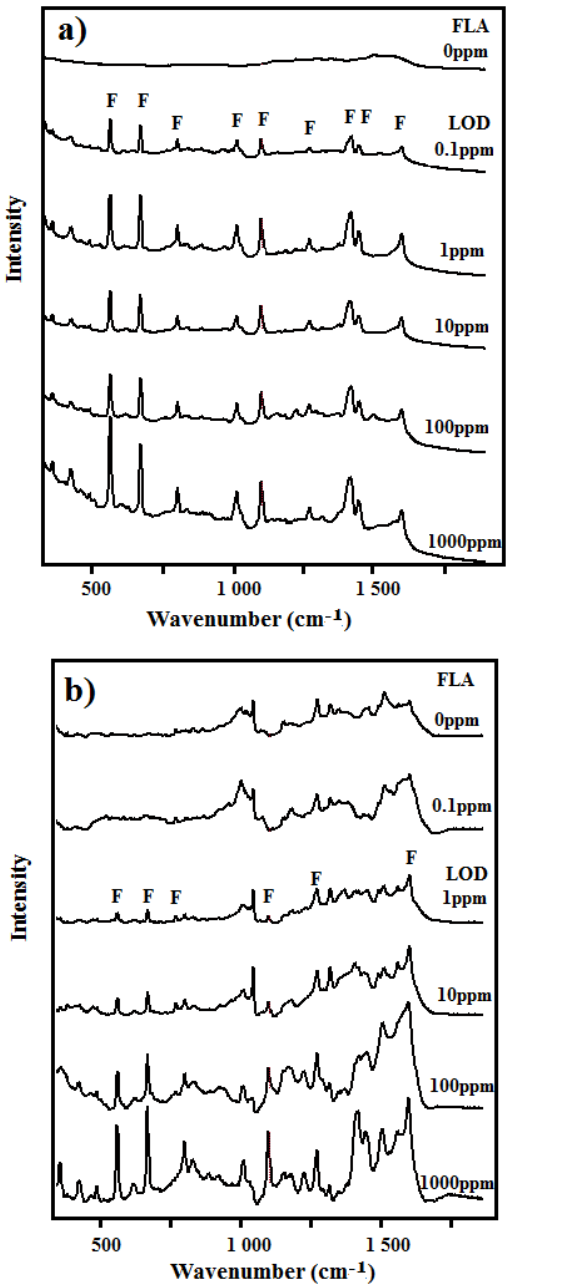

Figure 3. Spectra of fluoranthene in methanol in different concentrations between 0 ppm-1000 ppm on: a) CNP-Au (five different substrates); b) Ram-SERS-Au (same substrate). Λ=785 nm, laser power 10 mW, integration time 10 s. Background signal removing programs were not applied during preparation of this figure

Experimentally obtained LODs for all 16 EPA priority PAHs on conventional solid-support RAM-SERS-Au substrate and developed CNP-Au aggregation method as well as conventional Raman signals (from former studies [4]) are presented in the table below. Comparing experimental performance of the two substrates, we can see that overall LODs for CNP-Au (ranges between 0,001 ppm and 10 ppm) are three orders of magnitude lower than for RAM-SERS-Au (between 1 ppm and 1000 ppm). In two cases RAM-SERS-Au is not sensitive for a selected chemical (acenapthene and anthracene), while CNP-Au is

sensitive to all tested analytes. Only benzo[ghi]perylene and crysene have the same performance for both substrates (1 and 10 ppm, respectively), while in all other cases CNP-Au produces lower LODs. The best performance of the CNP-Au substrate compared to the Ram-SERS-Au is when measuring acenapthylene, where the sensitivity difference is four orders of magnitude. It should be noted, that SERS/Raman band shift of the same analyte on the different substrates (as well as comparing to conventional Raman) is expected, because of a chemisorption mechanism over physisorption. During chemisorption, the molecular structure of an adsorbate is modified due to the overlap of electron wave functions between analyte and metal colloids [32], resulting in slight Raman band shifts. Physisorpt molecules produce the same spectrum as free molecules except for their difference in bandwidth [9].

Table 1. Raman and SERS measurements of 16 EPA priority PAHs. Strong signals are in bold

PAH	No substrate, Raman shift, cm^{-1}	RAM-SERS-AU, Raman shift, cm^{-1}	RAM-SERS-AU LOD, ppm	CNP-Au, Raman shift, cm^{-1}	CNP-Au LOD, ppm
acenaphthene	Not measured	----------	Not sensitive	600 **642** 961 984 **1017 1214 1585**	0,1
acenaphthylene	Not measured	547 656 675 800 889 959 **999** 1027 1051 **1345 1424**	1000	**545** 654 **795 999** 1022 **1051 1325 1414**	0,1
anthracene	754 1008 1163 1186 1259 **1402** 1479 1555	----------	Not sensitive	754 1006 1161 1254 **1394** 1548	0,1
benz[a] anthracene	723 793 879 1008 1042 1166 1265 1321 1340 1392 1428 1559 1606	**356 718** 787 1027 1256 1337 1385 1421 1549	10	**355 718** 788 1028 1255 **1338** 1388 1427 1548	1
benzo[a]pyrene	1196 1212 **1234** 1343 **1384** 1581 1628	527 **609** 1234 1378	100	451 525 560 **608** 632 753 84 901 1015 **1234** 1344 **1379** 1569 1607	0,1
benzo[b] fluoranthene	Not measured	**393** 662 **687** 787 998 1014 1033 1189 1238 1378 1452 1624	10	**394** 415 589 675 **684** 783 993 1128 1188 1339 **1376** 1453 1585 1616	1
benzo[ghi] perylene	454 482 543 988 1083 1153 1222 1259 **1304 1389 1606**	389 **456** 483 541 1076 1254 1304 1387 1594	1	385 413 453 479 **539** 613 1074 **1253 1302 1385 1590**	1
benzo[k] fluoranthene	450 493 554 667 761 803 920 1025 1093 1272 1357 **1447** 1498 **1609**	452 **550** 667 756 798 915 1023 1087 1354 1437	10	450 **550** 667 760 798 914 1019 1085 1271 1360 **1436** 1590	1
chrysene	598 677 772 1019 **1383** 1431 1571	567 677 764 **1375** 1423	1	564 675 767 1011 **1375** 1424 1566	0,001
dibenz[ah] anthracene	Not measured	426 494 545 618 **717** 748 1031 1215 1295 **1343** 1432	100	328 43 496 546 617 750 716 1030 1213 194 **1341** 1427	1
fluoranthene	486 564 674 80 827 1022 **1103** 1136 1272 1370 **1421** 1457 1609	**560 664** 795 **1041** 1095 1268 1313 1364 1443 1504 1596	1	416 **560 669** 799 1010 **1097** 1268 **1417** 1449 1601	0,1
fluorene	418 **744** 844 1022 1149 1236 1291 1340 1392 1473 1609	603 822 1000 1145 1341 1550	10	**738** 783 862 **1019** 1151 **1219 1293** 1348 1477 **1530**	10
indeno[1,2,3-cd] pyrene	Not measured	408 513 581 628 678 998 **1237** 1418 1607	100	408 472 511 582 625 674 997 1185 1205 **1237 1416** 1605 1637	1
naphthalene	515 **765** 1022 **1385** 1460 1571	501 683 1146 **1268** 1381 1341 1442 1498	1	391 503 565 646 **853 898 998** 1238 1317 **1383** 1495	0,1
phenantrene	**712** 834 1039 1169 1245 **1350** 1437	543 **706** 827 1030 1198 1268 **1351** 1428 1600	100	404 543 **706** 827 1030 1200 1240 1350 1430 1600	0,1
pyrene	406 596 1066 1143 **1242 1405** 1593 1625	403 **588 1235** 1617	1	406 **589** 642 1016 1056 1137 **1235** 1401 1609	0,1

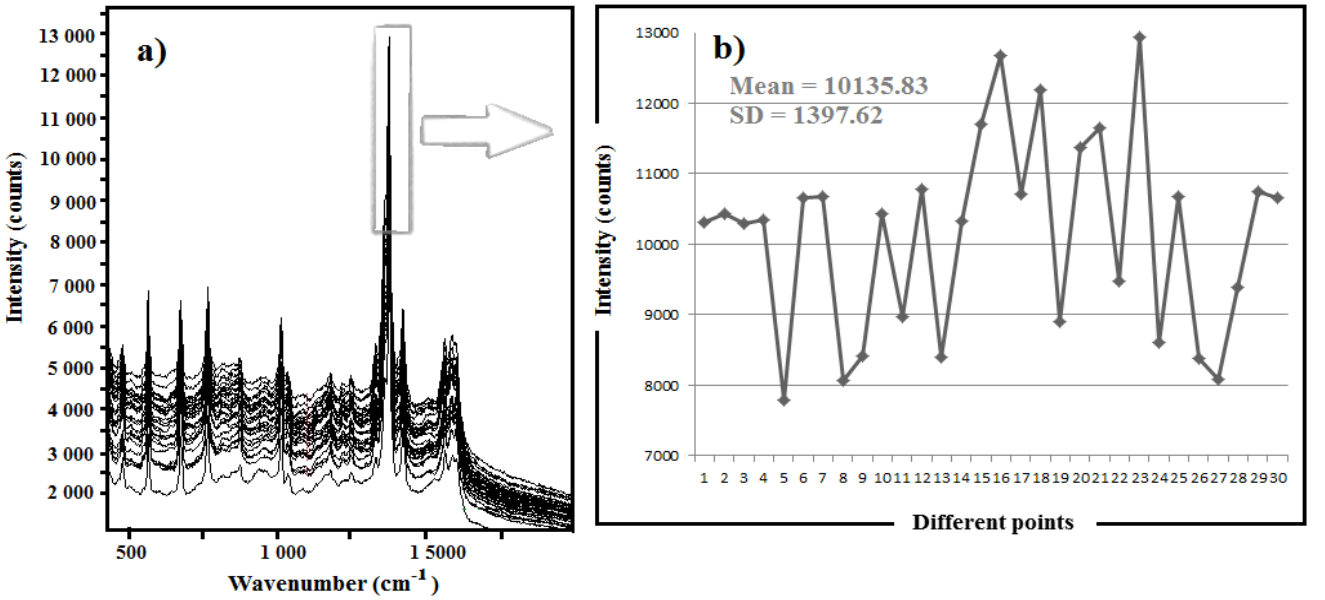

24

Figure 4. CNP-Au reproducibility experiment, a) SERS response of 1 ppb crysene in acetone on 30 randomly selected areas around crystal formations, b) different 1375 cm^{-1} Raman peak intensities. Λ= 785nm, laser power at the sample 10 mW, 10 s integration time

3.4. Reproducibility

For the purpose of determining reproducibility of SERS signal of the 1 ppb crysene on CNP-Au substrate, it was measured 30 times in different spots of the different substrates within the area of crystal formations (figure 4a). The intensities of the Raman peaks at 1375 cm^{-1} are plotted in figure 4b, with the mean value of 10135.83 counts and standard deviation 1397.62 counts (13.78%), which falls within the acceptable value of 20% [33].

4. Summary and Discussion

This study reports the application of gold nanoparticle suspensions, developed by a new method in comparison to conventional solid-support SERS substrates and is confirmed experimentally with the measurement of EPA's 16 priority PAHs. The novel method proposes prior mixing of the analyte with the substrate in a liquid form, followed by drying before each SERS measurement. This approach deceases experimental analyte detection limits up to three orders of magnitude compared to that from solid-support substrate (down to 1 ppb), as well as complete elimination of the background signal from the substrate. Reproducibility of the measurements is high (STD is below 14%). Apart from the advantages already listed, the application of this method is remarkably cost efficient due to the small amount of substrate needed for each measurement. This method does not replace previous studies, but offers a complimentary technique that can be used to attain a Raman signal in untargeted samples.

5. Limitations

The application of the described method has certain limitations. Due to a nonhomogeneous surface morphology, dried nanoparticles suspensions are not quantitative. Also it cannot be used for thermally unstable samples and in-situ applications may be limited.

Acknowledgements

The author gratefully acknowledges Prof. Chelsea Rochman from University of Toronto for professional support and allowing to use the laboratory and the Raman instrument; Prof. David Sinton (also from University of Toronto) for providing chemicals and consumables for the current study; Anne-Marie Dowgiallo from Ocean Optics for preparation of RAM-SERS-Au and CNP-Au substrates; as well as Jelena Grbic and James Chalmers for editing support.

REFERENCES

[1] H. I. Abdel-Shafy and M. S. M. Mansour, "A review on polycyclic aromatic hydrocarbons: Source, environmental impact, effect on human health and remediation," *Egyptian Journal of Petroleum*. 2016.

[2] J. R. Ferraro, K. Nakamoto, and C. W. Brown, *Introductory Raman Spectroscopy*. 2003.

[3] S. Lucht, T. Murphy, H. Schmidt, and H.-D. Kronfeldt, "Optimized recipe for sol-gel-based SERS substrates," *J. Raman Spectrosc.*, vol. 31, no. 11, pp. 1017–1022, Nov. 2000.

[4] A. Kolomijeca, "An autonomous sea going Raman/SERS instrument for in situ detection of chemicals in sea water (Book, 2013) [WorldCat.org]," Technical University Berlin, 2013.

[5] S.-Y. Ding, E.-M. You, Z.-Q. Tian, and M. Moskovits, "Electromagnetic theories of surface-enhanced Raman spectroscopy," *Chem. Soc. Rev.*, vol. 46, no. 13, pp. 4042–4076, Jul. 2017.

[6] A. Shiohara, Y. Wang, and L. M. Liz-Marzán, "Recent approaches toward creation of hot spots for SERS detection," *J. Photochem. Photobiol. C Photochem. Rev.*, vol. 21, pp. 2–25, Dec. 2014.

[7] P. Mosier-Boss, Mosier-Boss, and P. A., "Review of SERS Substrates for Chemical Sensing," *Nanomaterials*, vol. 7, no. 6, p. 142, Jun. 2017.

[8] F. Hu *et al.*, "Smart Liquid SERS Substrates based on Fe3O4/Au Nanoparticles with Reversibly Tunable Enhancement Factor for Practical Quantitative Detection," *Sci. Rep.*, vol. 4, no. 1, p. 7204, May 2015.

[9] Y.-H. Kwon, K. Sowoidnich, H. Schmidt, and H.-D. Kronfeldt, "Application of calixarene to high active surface-enhanced Raman scattering (SERS) substrates suitable for in situ detection of polycyclic aromatic hydrocarbons (PAHs) in seawater," *J. Raman Spectrosc.*, vol. 43, no. 8, pp. 1003–1009, Aug. 2012.

[10] A. Kolomijeca, Y.-H. Kwon, K. Sowoidnich, R. D. Prien, D. E. Schulz-Bull, and H.-D. Kronfeldt, "High sensitive Raman sensor for continuous in-situ detection of PAHs," in *Proceedings of the International Offshore and Polar Engineering Conference*, 2011.

[11] C. L. H. and and R. P. Van Duyne*, "Nanosphere Lithography: A Versatile Nanofabrication Tool for Studies of Size-Dependent Nanoparticle Optics," 2001.

[12] G. A. Baker and D. S. Moore, "Progress in plasmonic engineering of surface-enhanced Raman-scattering substrates toward ultra-trace analysis," *Anal. Bioanal. Chem.*, vol. 382, no. 8, pp. 1751–1770, Aug. 2005.

[13] R. Ossig, A. Kolomijeca, Y.-H. Kwon, F. Hubenthal, and H.-D. Kronfeldt, "SERS signal response and SERS/SERDS spectra of fluoranthene in water on naturally grown Ag nanoparticle ensembles," *J. Raman Spectrosc.*, vol. 44, no. 5, 2013.

[14] L. Wu *et al.*, "Highly sensitive, reproducible and uniform SERS substrates with a high density of three-dimensionally distributed hotspots: gyroid-structured Au periodic metallic materials," *NPG Asia Mater.*, vol. 10, no. 1, p. e462, Jan. 2018.

[15] A. Kolomijeca, H. D. Kronfeldt, and Y. H. Kwon, "A portable Surface Enhanced Raman Spectroscopy (SERS) Sensor System applied for seawater and sediment investigations on an Arctic sea-trial," *Int. J. Offshore Polar Eng.*, 2013.

[16] Y. H. Kwon, A. Kolomijeca, H. D. Kronfeldt, R. Ossig, and F. Hubenthal, "Naturally grown Ag nanoparticle SERS substrate as chemical sensor in fresh water applying 488 nm microsystem laser diode," *Int. J. Offshore Polar Eng.*, 2013.

[17] O. Péron, E. Rinnert, M. Lehaitre, P. Crassous, and C. Compère, "Detection of polycyclic aromatic hydrocarbon (PAH) compounds in artificial sea-water using surface-enhanced Raman scattering (SERS)," *Talanta*, vol. 79, no. 2, pp. 199–204, Jul. 2009.

[18] O. Péron, E. Rinnert, T. Toury, M. Lamy de la Chapelle, and C. Compère, "Quantitative SERS sensors for environmental analysis of naphthalene," *Analyst*, vol. 136, no. 5, pp. 1018–1022, Feb. 2011.

[19] H. Schmidt, N. Bich Ha, J. Pfannkuche, H. Amann, H.-D. Kronfeldt, and G. Kowalewska, "Detection of PAHs in seawater using surface-enhanced Raman scattering (SERS)," *Mar. Pollut. Bull.*, vol. 49, no. 3, pp. 229–234, Aug. 2004.

[20] L. G. Olson, R. H. Uibel, and J. M. Harris, "C18-Modified Metal-Colloid Substrates for Surface-Enhanced Raman Detection of Trace-Level Polycyclic Aromatic Hydrocarbons in Aqueous Solution," *Appl. Spectrosc.*, vol. 58, no. 12, pp. 1394–1400, Dec. 2004.

[21] L. Bao, P. Sheng, J. Li, S. Wu, Q. Cai, and S. Yao, "Surface enhanced Raman spectroscopic detection of polycyclic aromatic hydrocarbons (PAHs) using a gold nanoparticles-modified alginate gel network," *Analyst*, vol. 137, no. 17, p. 4010, Jul. 2012.

[22] X. Jiang, Y. Lai, M. Yang, H. Yang, W. Jiang, and J. Zhan, "Silver nanoparticle aggregates on copper foil for reliable quantitative SERS analysis of polycyclic aromatic hydrocarbons with a portable Raman spectrometer," *Analyst*, vol. 137, no. 17, p. 3995, Jul. 2012.

[23] Y. Xie *et al.*, "Selective SERS detection of each polycyclic aromatic hydrocarbon (PAH) in a mixture of five kinds of PAHs," *J. Raman Spectrosc.*, vol. 42, no. 5, pp. 945–950, May 2011.

[24] X. Shi, S. Liu, X. Han, J. Ma, Y. Jiang, and G. Yu, "High-Sensitivity Surface-Enhanced Raman Scattering (SERS) Substrate Based on a Gold Colloid Solution with a pH Change for Detection of Trace-Level Polycyclic Aromatic Hydrocarbons in Aqueous Solution," *Appl. Spectrosc.*, vol. 69, no. 5, pp. 574–579, May 2015.

[25] X. Shi, J. Ma, R. Zheng, C. Wang, and H.-D. Kronfeldt, "An improved self-assembly gold colloid film as surface-enhanced Raman substrate for detection of trace-level polycyclic aromatic hydrocarbons in aqueous solution," *J. Raman Spectrosc.*, vol. 43, no. 10, pp. 1354–1359, Oct. 2012.

[26] H. Wang, J. Zhao, A. M. D. Lee, H. Lui, and H. Zeng, "Improving skin Raman spectral quality by fluorescence photobleaching," *Photodiagnosis Photodyn. Ther.*, vol. 9, no. 4, pp. 299–302, Dec. 2012.

[27] K. Otto, C. P. Hubbard, W. H. Weber, and G. W. Graham, "Raman spectroscopy of palladium oxide on γ-alumina applicable to automotive catalysts: Nondestructive, quantitative analysis; oxidation kinetics; fluorescence quenching," *Appl. Catal. B Environ.*, vol. 1, no. 4, pp. 317–327, Dec. 1992.

[28] S. Yang *et al.*, "Laser Wavelength Dependence of Background Fluorescence in Raman Spectroscopic Analysis of Synovial Fluid from Symptomatic Joints.," *J. Raman Spectrosc.*, vol. 44, no. 8, pp. 1089–1095, Aug. 2013.

[29] J. Register, M. Maiwald, A. Fales, P. Strobbia, B. Sumpf, and T. Vo-Dinh, "Shifted-excitation Raman difference spectroscopy for the detection of SERS-encoded gold nanostar probes," *J. Raman Spectrosc.*, vol. 49, no. 12, pp. 1961–1967, Dec. 2018.

[30] P. C. Lee and D. Meisel, "Adsorption and surface-enhanced Raman of dyes on silver and gold sols," *J. Phys. Chem.*, vol. 86, no. 17, pp. 3391–3395, Aug. 1982.

[31] E. P. Hoppmann, W. W. Yu, and I. M. White, "Highly sensitive and flexible inkjet printed SERS sensors on paper," *Methods*, vol. 63, no. 3, pp. 219–224, Oct. 2013.

[32] A. Campion and P. Kambhampati, "Surface-enhanced Raman scattering," *Chem. Soc. Rev.*, vol. 27, no. 4, p. 241, Jan. 1998.

[33] U. S. Dinish, F. C. Yaw, A. Agarwal, and M. Olivo, "Development of highly reproducible nanogap SERS substrates: Comparative performance analysis and its application for glucose sensing," *Biosens. Bioelectron.*, vol. 26, no. 5, pp. 1987–1992, Jan. 2011.